

## MID-INFRARED OBSERVATIONS OF CLASS I/FLAT-SPECTRUM SYSTEMS IN SIX NEARBY MOLECULAR CLOUDS

KARL E. HAISCH, JR.<sup>1,2</sup>

Department of Physics, Utah Valley State College, 800 West University Parkway, Orem, UT 84058-5999; haischka@uvsc.edu

MARY BARSONY<sup>1,2,3,4</sup>

Department of Physics and Astronomy, San Francisco State University, 1600 Holloway Drive, San Francisco, CA 94132;  
mbarsony@stars.sfsu.edu

MICHAEL E. RESSLER<sup>1</sup>

Jet Propulsion Laboratory, Mail Stop 169-327, 4800 Oak Grove Drive, Pasadena, CA 91109; michael.e.ressler@jpl.nasa.gov

AND

THOMAS P. GREENE

NASA Ames Research Center, Mail Stop 245-6, Moffett Field, CA 94035-1000; tgreene@mail.arc.nasa.gov

Received 2006 January 23; accepted 2006 August 26

### ABSTRACT

We have obtained new mid-infrared observations of 65 Class I/flat-spectrum (FS) objects in the Perseus, Taurus, Chamaeleon I and II,  $\rho$  Ophiuchi, and Serpens dark clouds. These objects represent a subset of the young stellar objects (YSOs) from our previous near-infrared multiplicity surveys. We detected 45 out of 48 (94%) of the single sources, 16 out of 16 (100%) of the primary components, and 12 out of 16 (75%) of the secondary/triple components of the binary/multiple objects surveyed. One target, IRS 34, a  $0''.31$  separation FS binary, remains unresolved at near-infrared wavelengths. The composite spectral energy distributions for all of our sample YSOs are either Class I or FS, and in 15 out of 16 multiple systems at least one of the individual components displays a Class I or FS spectral index. However, the occurrence of mixed pairings, such as FS with Class I, FS with Class II, and, in one case, an FS with a Class III (Cha I T33B), is surprisingly frequent. Such behavior is not consistent with that of multiple systems among T Tauri stars (TTSs), where the companion of a classical TTS also tends to be a classical TTS, although other mixed pairings have been previously observed among Class II YSOs. Based on an analysis of the spectral indices of the individual binary components, there appears to be a higher proportion of mixed Class I/FS systems (65%–80%) than that of mixed classical and weak-lined TTSs (25%–40%), demonstrating that the envelopes of Class I/FS systems are rapidly evolving during this evolutionary phase. In general, the individual binary/multiple components suffer very similar extinctions,  $A_v$ , suggesting that most of the line-of-sight material is either in the foreground of the molecular cloud or circumbinary. We report the discovery of a steep spectral index secondary companion to ISO-Cha I 97, detected for the first time via our mid-infrared observations. In our previous near-infrared imaging survey of binary/multiple Class I and FS YSOs, ISO-Cha I 97 appeared to be single. With a spectral index of  $\alpha \geq +3.9$ , the secondary component of this system is a member of a rare class of very steep spectral index YSOs, those with  $\alpha > +3$ . Only three such objects have previously been reported, all of which are either Class 0 or Class I.

*Key words:* binaries: close — stars: formation — stars: pre-main-sequence

### 1. INTRODUCTION

We have known for many years that the majority of solar-to-late-type field stars are binaries or multiples (Abt & Levy 1976; Duquennoy & Mayor 1991; Fischer & Marcy 1992), but only in the past decade have significant numbers of pre-main-sequence (PMS) stars been surveyed for multiplicity. Near-infrared surveys of nearby, young dark cloud complexes have shown that young, low-mass T Tauri stars (TTSs) have binary fractions that are greater than or equal to that of the field (e.g., Ghez et al. 1993, 1997; Mathieu 1994; Simon et al. 1995; Barsony

et al. 2003) and appear to be coeval, that is, at the same evolutionary age (Hartigan et al. 1994; Brandner & Zinnecker 1997). Observations at millimeter continuum wavelengths also find multiple sources at the origins of extended molecular outflows and optical jets (Looney et al. 1997). Thus, the formation of binary and multiple systems appears to be the rule, rather than the exception, in star-forming regions.

Recently, multiplicity surveys have been extended to include even younger, self-embedded young stellar objects (YSOs), those with Class I and flat-spectrum spectral energy distributions (SEDs; Lada 1987; Adams et al. 1987, 1988). The first survey for multiplicity among such objects was conducted by Looney et al. (2000) with the BIMA millimeter interferometer at 2.7 mm. Of the eight Class 0 and Class I YSOs surveyed, all were members of binary systems or small groups. Not long thereafter, Reipurth (2000) analyzed the multiplicity of 14 young (ages  $\leq 10^5$  yr) sources that drive giant Herbig-Haro flows. Between 79% and 86% (depending on the range of separations considered) of these sources had at least one companion, and of these half

<sup>1</sup> Observations with the Palomar 5 m telescope were obtained under a collaborative agreement between Palomar Observatory and the Jet Propulsion Laboratory.

<sup>2</sup> Visiting Astronomer at the Baade telescope of the Magellan Observatory, a joint facility of the Carnegie Observatories, Harvard University, Massachusetts Institute of Technology, the University of Arizona, and the University of Michigan.

<sup>3</sup> Space Science Institute, 4750 Walnut Street, Suite 205, Boulder, CO 80301.

<sup>4</sup> NASA Faculty Fellow.

TABLE 1  
MID-INFRARED 10  $\mu\text{m}$  FLUXES FOR MULTIPLE SOURCES

Source (1)	R.A. (J2000.0) (2)	Decl. (J2000.0) (3)	$F_{10 \mu\text{m}}$ (Jy) (4)	Obs. Date (5)	Tel./Inst. <sup>a</sup> (6)
03260+3111 <sup>b</sup> .....	03 29 10.40	+31 21 58.0	0.751	2003 Dec 17	P200/MIRLIN
Secondary.....	03 29 10.61	+31 22 00.43	$\leq 0.12$	2003 Dec 17	P200/MIRLIN
Cha I T33B.....	11 08 15.69	-77 33 47.1	5.96	2003 Mar 17	M6.5m/MIRAC
Secondary.....	11 08 14.98	-77 33 46.5	$\leq 0.045$	2003 Mar 17	M6.5m/MIRAC
Ced 110 IRS6.....	11 07 09.80	-77 23 04.4	0.210	2003 Mar 17	M6.5m/MIRAC
Secondary.....	11 07 10.40	-77 23 04.6	0.077	2003 Mar 17	M6.5m/MIRAC
ISO-Cha I 97.....	11 07 18.30	-77 23 13.0	0.210	2003 Mar 17	M6.5m/MIRAC
Secondary.....	11 07 18.90	-77 23 13.6	0.048	2003 Mar 17	M6.5m/MIRAC
GY 23.....	16 26 24.00	-24 24 49.9	2.02	1998 Jul 2	P200/MIRLIN
GY 21.....	16 26 23.54	-24 24 41.5	0.40	1998 Jul 2	P200/MIRLIN
IRS 48.....	16 27 37.20	-24 30 34.0	3.91	1998 Jun 30	P200/MIRLIN
IRS 50.....	16 27 38.10	-24 30 40.0	$\leq 0.097$	1998 Jul 1	P200/MIRLIN
L1689 SNO2.....	16 31 52.13	-24 56 15.2	1.95	2003 Mar 17	M6.5m/MIRAC
Secondary.....	16 31 51.94	-24 56 13.7	0.213	2003 Mar 17	M6.5m/MIRAC
IRS 51.....	16 27 39.84	-24 43 16.1	0.730	1997 Jun 25	P200/MIRLIN
Secondary.....	16 27 39.86	-24 43 17.5	0.480	1997 Jun 25	P200/MIRLIN
IRS 43.....	16 27 26.90	-24 40 51.5	1.54	1998 Jun 7	KeckII/MIRLIN
Secondary.....	16 27 26.88	-24 40 51.1	0.52	1998 Jun 7	KeckII/MIRLIN
GY 263.....	16 27 26.60	-24 40 45.9	0.030	1998 Jun 7	KeckII/MIRLIN
IRS 54 <sup>c</sup> .....	16 27 51.70	-24 31 46.0	2.51	1997 Jun 26	P200/MIRLIN
Secondary.....	16 27 51.39	-24 31 40.1	$\leq 0.045$	1997 Jun 26	P200/MIRLIN
GY 51.....	16 26 30.49	-24 22 59.0	0.224	1998 Jun 7	KeckII/MIRLIN
Secondary.....	16 26 30.57	-24 22 59.5	$\leq 0.018$	1998 Jun 7	KeckII/MIRLIN
Tertiary.....	16 26 30.90	-24 22 58.2	$\leq 0.018$	1998 Jun 7	KeckII/MIRLIN
WL 1.....	16 27 04.13	-24 28 30.7	0.08	1998 Jun 7	KeckII/MIRLIN
Secondary.....	16 27 04.09	-24 28 30.1	0.05	1998 Jun 7	KeckII/MIRLIN
WL 2.....	16 26 48.56	-24 28 40.4	0.139	1998 Jun 7	KeckII/MIRLIN
Secondary.....	16 26 48.47	-24 28 36.4	0.016	1998 Jun 7	KeckII/MIRLIN
GY 244.....	16 27 17.54	-24 28 56.5	0.194	1996 Apr 24	P200/MIRLIN
WL 5.....	16 27 18.00	-24 28 55.0	0.050 <sup>d</sup>	1999 Jun 28	KeckI/LWS
IRS 34 <sup>e</sup> .....	16 27 15.48	-24 26 40.6	0.092	1998 Jun 7	KeckII/MIRLIN
Secondary.....	16 27 15.46	-24 26 40.8	0.080	1998 Jun 7	KeckII/MIRLIN
SVS 20.....	18 29 57.70	+01 14 07.0	4.36	1998 Jun 7	KeckII/MIRLIN
Secondary.....	18 29 57.72	+01 14 08.5	1.53	1998 Jun 7	KeckII/MIRLIN
EC 95.....	18 29 57.80	+01 12 52.0	0.100	1998 Jun 7	KeckII/MIRLIN
EC 92.....	18 29 57.75	+01 12 57.0	0.550	1998 Jun 7	KeckII/MIRLIN

NOTE.—Units of right ascension are hours, minutes, and seconds, and units of declination are degrees, arcminutes, and arcseconds.

<sup>a</sup> P200, Palomar 200 inch (5 m) telescope; M6.5m, Magellan 6.5 m telescope; LWS, Long Wavelength Spectrometer. P200/MIRLIN, KeckII/MIRLIN, and KeckI/LWS data for all objects listed in this table are from Barsony et al. (2005).

<sup>b</sup> 03260+3111 was resolved in the near-infrared with a  $3''.26$  separation at P.A.  $47^\circ 9'$  (Haisch et al. 2004). The source is unresolved but extended with a fan-shaped nebulosity in the mid-infrared.

<sup>c</sup> IRS 54 is a binary source in the near-infrared, but the secondary was not detected in the mid-infrared.

<sup>d</sup> Flux listed for WL 5 is at  $12.5 \mu\text{m}$ .

<sup>e</sup> IRS 34 was not resolved in the near-infrared due to the tight separation ( $0''.31$ ) and faintness of the individual components.

were higher order multiple systems. These fractions are even larger than those found among either the PMS TTSs or field-star populations.

In order to determine the multiplicity properties of embedded Class I and flat-spectrum sources with reasonable statistical confidence, which the previous surveys do not provide, Haisch et al. (2002, 2004) and Duchêne et al. (2004) conducted the first near-infrared imaging surveys of nearby molecular clouds, which permitted observations at resolutions  $\leq 1''$  and therefore enabled detections of companions as close as 100–300 AU, depending on the distance to the clouds. Merging the three surveys into one, these authors derived a “restricted” companion star fraction ( $\Delta K \leq 4$  mag and a separation range of 300–1400 AU) of  $16\% \pm 3\%$ , with all clouds presenting fully consistent fractions. This frequency is in excellent agreement with that obtained for

TTSs in the same star-forming regions and is approximately twice as high as that observed for late-type field dwarfs.

While near-infrared data are very efficient in identifying binary/multiple components, such observations are not at a long enough wavelength to determine the evolutionary state of the objects via their spectral indices (as defined in § 3). However, since contamination from photospheric emission is minimal at mid-infrared wavelengths, observations at  $10 \mu\text{m}$ , in conjunction with near-infrared *JHKL* data, can be used to ascertain the spectral index and thus the evolutionary state of the individual binary/multiple YSOs. The  $10 \mu\text{m}$  radiation from each component does not originate from the star itself but from a “photosphere” of surrounding dust heated to several hundred degrees. Radiative transfer models of Class I YSOs have shown that the  $10 \mu\text{m}$  photosphere is located about 1 AU from a low-mass protostar (e.g., Kenyon

TABLE 2  
MID-INFRARED 10  $\mu\text{m}$  FLUXES FOR SINGLE PERSEUS SOURCES

Source (1)	R.A. (J2000.0) (2)	Decl. (J2000.0) (3)	$F_{10\ \mu\text{m}}$ (Jy) (4)	Obs. Date (5)	Tel./Inst. <sup>a</sup> (6)
03382+3145 .....	03 41 22.70	+31 54 46.0	$\leq 0.031$	2003 Dec 17	P200/MIRLIN
03259+3105 .....	03 29 03.70	+31 15 52.0	7.24	2003 Dec 17	P200/MIRLIN
03262+3114 .....	03 29 20.40	+31 24 47.0	$\leq 0.024$	2003 Dec 17	P200/MIRLIN
03380+3135 .....	03 41 09.10	+31 44 38.0	0.244	2003 Dec 17	P200/MIRLIN
03220+3035 .....	03 25 09.20	+30 46 21.0	0.328	2003 Dec 17	P200/MIRLIN
03254+3050 .....	03 28 35.10	+31 00 51.0	0.219	2003 Dec 17	P200/MIRLIN
03445+3242 .....	03 47 41.60	+32 51 43.5	1.05	2003 Dec 17	P200/MIRLIN
03439+3233 .....	03 47 05.00	+32 43 09.0	0.199	2003 Dec 17	P200/MIRLIN

NOTE.—Units of right ascension are hours, minutes, and seconds, and units of declination are degrees, arcminutes, and arcseconds.

<sup>a</sup> P200, Palomar 200 inch telescope.

et al. 1993; Chick & Cassen 1997). Thus, the individual components should be point sources in the mid-infrared. Indeed, recent 10  $\mu\text{m}$  observations of Class I objects have often found them to be unresolved (e.g., Barsony et al. 2005). Finally, no current space-based observatory can match the angular resolution achievable from the ground at mid-infrared wavelengths, which is ideal for studying very young binaries.

Mid-infrared studies of small samples of Class I/flat-spectrum binaries have already been published (Liu et al. 1996; Girart et al. 2004; Ciardi et al. 2003). In this paper, we present the results of a mid-infrared imaging survey of 65 single and binary/multiple Class I and flat-spectrum YSOs from our previous near-infrared surveys (Haisch et al. 2002, 2004) in the  $\rho$  Ophiuchus ( $d = 125$  pc; Knude & Høg 1998), Serpens ( $d = 310$  pc; de Lara et al. 1991), Taurus ( $d = 140$  pc; Kenyon & Hartmann 1995), Perseus ( $d = 320$  pc; Herbig 1998), and Chamaeleon I and II ( $d = 160$  and 178 pc; Whittet et al. 1997) star-forming regions, respectively. Following the near-infrared multiplicity survey of Haisch et al. (2004), we impose a lower limit for detectable separations of 100–140 AU for Tau, Cha, and  $\rho$  Oph and  $\sim 300$  AU for Per and Ser, which was set by the seeing in the near-infrared. We have also imposed an upper limit to the separations of 2000 AU in order to avoid including sources that are not gravitationally bound systems (e.g., Reipurth & Zinnecker 1993; Simon et al. 1995). In addition, sensitivity calculations from our near-infrared data indicate that we can detect a  $K = 4$  mag difference between the

primary and companion at a separation of  $1''$  at the  $5\sigma$  confidence level. Thus, we restrict our analysis to component magnitude differences  $\Delta K \leq 4$  mag. We discuss our mid-infrared observations and data reduction procedures in § 2. In § 3 we present the results of our survey, and we discuss the results in § 4. We summarize our primary results in § 5.

## 2. OBSERVATIONS AND DATA REDUCTION

The mid-infrared imaging data for this survey were obtained with MIRLIN, the Jet Propulsion Laboratory's  $128 \times 128$  pixel Si:As camera (Ressler et al. 1994), and MIRAC3/BLINC, a mid-infrared array camera built for astronomical imaging at the Steward Observatory, University of Arizona, and the Harvard Smithsonian Center for Astrophysics (Hoffmann et al. 1998). MIRAC3/BLINC uses a Rockwell HF-16  $128 \times 128$  pixel Si:As BIB hybrid array. All observations at Palomar were made with MIRLIN, whereas MIRAC3/BLINC was used on the Baade 6.5 m telescope.

Mid-infrared  $N$ -band ( $\lambda_0 = 10.78\ \mu\text{m}$ ,  $\Delta\lambda = 5.7\ \mu\text{m}$ ) observations of all Tau and Per sources were obtained with MIRLIN on 2003 December 17. Observations at  $N$  band ( $\lambda_0 = 10.3\ \mu\text{m}$ ,  $\Delta\lambda = 1.03\ \mu\text{m}$ ) of all sources in Cha I and L1689 SNO2 and IRS 67 in  $\rho$  Oph were obtained with MIRAC3/BLINC during the period 2003 March 17–19. Fluxes for the remaining  $\rho$  Oph sources surveyed were taken from Barsony et al. (2005). MIRLIN has a plate scale of  $0''.15\ \text{pixel}^{-1}$  and a  $19''.2 \times 19''.2$  field of view

TABLE 3  
MID-INFRARED 10  $\mu\text{m}$  FLUXES FOR SINGLE TAURUS SOURCES

Source (1)	R.A. (J2000.0) (2)	Decl. (J2000.0) (3)	$F_{10\ \mu\text{m}}$ (Jy) (4)	Obs. Date (5)	Tel./Inst. <sup>a</sup> (6)
Haro 6-13 .....	04 32 15.61	+24 29 02.3	1.39	2003 Dec 17	P200/MIRLIN
Haro 6-28 .....	04 35 55.87	+22 54 35.5	0.089	2003 Dec 17	P200/MIRLIN
04489+3042 .....	04 52 06.90	+30 47 17.0	0.278	2003 Dec 17	P200/MIRLIN
04016+2610 .....	04 04 42.85	+26 18 56.3	2.46	2003 Dec 17	P200/MIRLIN
04108+2803A <sup>b</sup> .....	04 13 52.90	+28 11 23.0	0.839	2003 Dec 17	P200/MIRLIN
04361+2547 .....	04 39 13.87	+25 53 20.6	0.724	2003 Dec 17	P200/MIRLIN
04365+2535 .....	04 39 35.01	+25 41 45.5	0.972	2003 Dec 17	P200/MIRLIN
04295+2251 .....	04 32 32.10	+22 57 30.0	0.391	2003 Dec 17	P200/MIRLIN
04264+2433 .....	04 29 30.30	+24 39 54.0	0.432	2003 Dec 17	P200/MIRLIN

NOTE.—Units of right ascension are hours, minutes, and seconds, and units of declination are degrees, arcminutes, and arcseconds.

<sup>a</sup> P200, Palomar 200 inch telescope.

<sup>b</sup> The Class I object, IRAS 04108+2803B ( $\alpha_{2000.0} = 04^{\text{h}}13^{\text{m}}54^{\text{s}}.69$ ,  $\delta_{2000.0} = 28^{\circ}11'33''.1$ ), at  $21''$  separation from 04108+2803A, falls outside our 2000 AU separation limit, but the pair have been considered to be a binary system by previous authors (e.g., Barsony & Kenyon 1992).

TABLE 4  
MID-INFRARED 10  $\mu\text{m}$  FLUXES FOR SINGLE CHAMAELEON SOURCES

Source (1)	R.A. (J2000.0) (2)	Decl. (J2000.0) (3)	$F_{10\ \mu\text{m}}$ (Jy) (4)	Obs. Date (5)	Tel./Inst. <sup>a</sup> (6)
Cha I T32.....	11 08 04.61	-77 39 16.9	2.99	2003 Mar 17	M6.5m/MIRAC
Cha I T44.....	11 10 01.35	-76 34 55.8	3.88	2003 Mar 17	M6.5m/MIRAC
Cha I T42.....	11 09 54 66	-76 34 23.7	5.82	2003 Mar 17	M6.5m/MIRAC
Cha I T29.....	11 07 59.25	-77 38 43.9	3.66	2003 Mar 17	M6.5m/MIRAC
ISO-Cha I 26 .....	11 08 04.00	-77 38 42.0	0.790	2003 Mar 19	M6.5m/MIRAC
Cha I C1-6 .....	11 09 23.30	-76 34 36.2	0.910	2003 Mar 17	M6.5m/MIRAC
Cha I C9-2 .....	11 08 37.37	-77 43 53.5	4.01	2003 Mar 17	M6.5m/MIRAC

NOTE.— Units of right ascension are hours, minutes, and seconds, and units of declination are degrees, arcminutes, and arcseconds.

<sup>a</sup> M6.5m, Magellan 6.5 m telescope.

at the Palomar 5 m telescope. At the Baade 6.5 m telescope, MIRAC3/BLINC has a plate scale of  $0''.123\ \text{pixel}^{-1}$  and a  $15''.7 \times 15''.7$  field of view. For reference, the full width at half-maximum of a diffraction-limited image at  $N$  band with MIRLIN is  $0''.47$  at the Palomar 5 m telescope; the corresponding value with MIRAC3/BLINC is  $0''.40$  at the Baade 6.5 m telescope.

Standard mid-infrared chop-nod techniques were used for the data acquisition. For all MIRLIN and MIRAC3/BLINC observations, the telescope's secondary mirror was chopped  $8''$  in a north-south direction, at a rate of a few hertz. In order to remove residual differences in the background level, the entire telescope was nodded  $8''$  east-west. Several hundred co-added chop pairs, with 5–6 ms integration times per frame, were com-

bined to produce images with a total on-source integration time of 25 s with MIRLIN and 60 s with MIRAC3/BLINC.

All MIRAC3/BLINC data were reduced using the Image Reduction and Analysis Facility (IRAF).<sup>5</sup> All target frames were background-subtracted, shifted, and co-added to produce the final images of each object. For the MIRLIN data, all raw images were background-subtracted, shifted, and co-added with our in-house IDL routine, “mac” (match and combine).

<sup>5</sup> IRAF is distributed by the National Optical Astronomy Observatory, which is operated by the Association of Universities for Research in Astronomy, Inc., under cooperative agreement with the National Science Foundation.

TABLE 5  
MID-INFRARED 10  $\mu\text{m}$  FLUXES FOR SINGLE  $\rho$  OPH SOURCES

Source (1)	R.A. (J2000.0) (2)	Decl. (J2000.0) (3)	$F_{10\ \mu\text{m}}^{\text{a}}$ (Jy) (4)	Obs. Date (5)	Tel./Inst. <sup>b</sup> (6)
Elias 29 .....	16 27 09.43	-24 37 18.5	23.7	1997 Jun 26	P200/MIRLIN
IRS 42.....	16 27 21.45	-24 41 42.8	2.03	1997 Jun 27	P200/MIRLIN
GSS 30/IRS 1 .....	16 26 21.50	-24 23 07.0	8.17	1998 Jun 30	P200/MIRLIN
GY 279 .....	16 27 30.18	-24 27 44.3	0.954	1997 Jun 27	P200/MIRLIN
IRS 63.....	16 31 35.53	-24 01 28.3	0.948	2003 Mar 17	M6.5m/MIRAC
GSS 26.....	16 26 10.28	-24 20 56.6	1.01	1997 Jun 27	P200/MIRLIN
WL 17.....	16 27 06.79	-24 38 14.6	0.825 <sup>c</sup>	1999 Jun 29	KeckI/LWS
IRS 67.....	16 32 01.00	-24 56 44.0	0.822	2003 Mar 17	M6.5m/MIRAC
WL 12.....	16 26 44.30	-24 34 47.5	1.14	1998 Jul 1	P200/MIRLIN
IRS 44.....	16 27 28.00	-24 39 34.3	2.65	1997 Jun 27	P200/MIRLIN
IRS 46.....	16 27 29.70	-24 39 16.0	0.540	1998 Jun 7	KeckII/MIRLIN
WL 6.....	16 27 21.83	-24 29 53.2	1.01	1998 Jun 7	KeckII/MIRLIN
GY 224 .....	16 27 11.17	-24 40 46.7	0.255	1998 Jun 7	KeckII/MIRLIN
WL 19.....	16 27 11.74	-24 38 32.1	0.130	1996 Apr 24	P200/MIRLIN
WL 3.....	16 27 19.30	-24 28 45.0	0.162	1997 Jun 27	P200/MIRLIN
CRBR 15 .....	16 26 19.30	-24 24 16.0	0.074 <sup>c</sup>	1999 Jun 28	KeckI/LWS
CRBR 12 .....	16 26 17.30	-24 23 49.0	0.315	1997 Jun 27	P200/MIRLIN
GY 344 .....	16 27 45.81	-24 44 53.7	0.117 <sup>c</sup>	1999 Jun 28	KeckI/LWS
IRS 33.....	16 27 14.60	-24 26 55.0	0.062	1998 Jun 7	KeckII/MIRLIN
GY 245 .....	16 27 18.50	-24 39 15.0	0.068	1998 Jun 7	KeckII/MIRLIN
CRBR 85 .....	16 27 24.68	-24 41 03.7	0.216	1997 Jun 27	P200/MIRLIN
GY 91.....	16 26 40.60	-24 27 16.0	0.157	1997 Jun 27	P200/MIRLIN
WL 22.....	16 26 59.30	-24 35 01.0	0.443	1998 Jun 30	P200/MIRLIN
GY 197 .....	16 27 05.40	-24 36 31.0	$\leq 0.042$	1998 Jun 30	P200/MIRLIN

NOTE.— Units of right ascension are hours, minutes, and seconds, and units of declination are degrees, arcminutes, and arcseconds.

<sup>a</sup> MIRLIN and LWS fluxes taken from Barsony et al. (2005).

<sup>b</sup> P200, Palomar 200 inch telescope; M6.5m, Magellan 6.5 m telescope.

<sup>c</sup> The fluxes listed for WL 17, CRBR 15, and GY 344 are 12.5  $\mu\text{m}$  fluxes.

TABLE 6  
 COLORS, SPECTRAL INDICES, AND EXTINCTION ESTIMATES FOR MULTIPLE SOURCES

Source	$K$	$(J - H)$	$(H - K)$	$(K - L)$	$(K - N)$	$\alpha$	SED	$A_v$
03260+3111.....	7.29	1.28	0.79	0.54	3.17	-0.91	II	6.5
	11.04	1.54	1.03	0.82	<3.44	<-0.84	II-III	6.8
Cha I T33B.....	6.93	1.22	1.17	...	1.93	+0.13	FS	2.6
	8.85	0.82	0.31	...	<1.62	$\leq -1.89$	III	3.2
Ced 110 IRS6.....	10.86	>4.82	4.32	...	5.30	+0.30	FS	$\geq 51.0$
	12.86	>2.43	4.71	...	6.21	0.85	I	...
ISO-Cha I 97.....	11.20	...	...	...	5.64	+0.50	I	...
	...	...	...	...	...	$\geq +3.90$	0(?)	...
GY 23.....	7.39	2.15	1.20	1.47	4.34	-0.36	II	11.0
GY 21.....	10.09	2.72	1.78	2.05	5.29	+0.13	FS	16.0
IRS 48.....	7.71	1.68	1.01	1.59	5.38	+0.26	FS	6.8
IRS 50.....	9.92	1.60	1.02	0.68	<3.58	$\leq -0.68$	II	8.5
L1689 SNO2.....	8.32	2.35	1.49	1.68	5.18	+0.20	FS	12.0
	8.86	2.08	1.19	0.90	3.31	-0.88	II	14.0
IRS 51.....	8.69	6.56	2.35	1.81	4.54	-0.29	FS	34.0
	11.18	>7.12	1.47	2.01	6.57	+0.94	I	...
IRS 43.....	9.44	>6.70	3.12	2.67	6.10	+0.54	I	...
GY 263.....	12.42	>5.10	1.77	1.71	4.80	-0.12	FS	$\geq 38.0$
IRS 54.....	10.15	4.16	2.07	2.41	7.34	+1.45	I	...
	14.29	>3.87	1.84	1.15	<7.11	$\leq +1.49$	I	...
GY 51.....	10.16	4.19	2.06	2.00	4.73	-0.18	FS	30.0
	11.09	3.99	1.90	1.67	<2.92	$\leq -1.28$	II	31.0
	15.51	>2.73	1.76	<2.01	<7.34	$\leq +1.49$	I	...
WL 1 <sup>a</sup> .....	10.76	4.37	2.08	1.74	4.21	-0.49	II	35.0
	10.85	4.32	2.06	1.67	3.79	-0.74	II	33.0
WL 2.....	11.15	5.31	2.80	2.80	5.20	+0.10	FS	38.0
	12.42	4.92	2.73	1.82	4.12	-0.56	II	38.0
GY 244.....	10.94	4.76	3.52	2.40	5.35	+0.11	FS	33.0
WL 5.....	10.21	>5.47	4.82	2.27	<2.59	<-1.61	III	$\geq 44.0$
SVS 20.....	7.09	3.46	1.65	1.75	4.88	-0.07	FS	24.0
	8.38	3.66	1.92	2.09	5.03	-0.03	FS	22.0
EC 95.....	9.78	4.03	2.12	1.44	3.47	-0.90	II	32.0
EC 92.....	10.44	2.68	1.59	1.48	5.98	+0.66	I	...

<sup>a</sup> WL1 has a flat-spectrum spectral index in Bontemps et al. (2001) and was resolved into binary Class II components by Barsony et al. (2005).

Flux calibration was performed using  $\alpha$  Tau ( $N = -3.02$ ) as our standard star for the MIRLIN observations and both  $\alpha$  CMA ( $N = -1.35$ ) and  $\gamma$  Cru ( $N = -3.36$ ) for the MIRAC3/BLINC data. The standards were observed on the same nights and through the same range of air masses as the target sources. Zero points and extinction coefficients were established for each night using a straight-line fit to the instrumental minus true magnitudes of the standards as a function of air mass. Typical air-mass corrections for the MIRLIN data were of order  $0.5 \text{ mag air mass}^{-1}$ , while the corrections for the MIRAC3/BLINC data were of order  $0.1\text{--}0.2 \text{ mag air mass}^{-1}$ . By adding the errors in the zero-point offsets, the air-mass corrections, the aperture corrections, and the magnitudes of the standards in quadrature and taking the square root, we estimate that the total photometric uncertainty for the MIRLIN observations is typically good to within  $\pm 0.10 \text{ mag}$ , and  $\pm 0.06$  for the MIRAC3/BLINC data. Typical  $1 \sigma$   $10 \mu\text{m}$  rms sensitivities were  $0.040 \text{ Jy}$  with both MIRLIN at Palomar and MIRAC at Magellan. Note that  $0.00 \text{ mag}$  at  $N$  band with MIRLIN corresponds to  $33.4 \text{ Jy}$ , whereas  $0.00 \text{ mag}$  with MIRAC3/BLINC corresponds to  $35.2 \text{ Jy}$ .

Aperture photometry was performed for the MIRLIN data using  $14 \text{ pixel}$  ( $2''.1$ ) radii for standards and  $8 \text{ pixel}$  ( $1''.2$ ) radii for program objects. The corresponding apertures used for the MIRAC3/BLINC photometry had  $10 \text{ pixel}$  ( $1''.2$ ) and  $6 \text{ pixel}$  ( $0''.7$ ) radii for the standards and program objects, respectively. Sky values around each source were determined from the mode of

intensities in an annulus with a radius of  $3 \text{ pixels}$  ( $0''.36$  and  $0''.45$  for MIRAC and MIRLIN, respectively). Our choice of aperture size for our target photometry ensured that the individual source fluxes were not contaminated by the flux from companion stars; however, they are not large enough to include all the flux from a given source. In order to account for this missing flux, aperture corrections were derived from the flux standards, and the instrumental magnitudes for all sources were corrected to account for the missing flux.

### 3. ANALYSIS AND RESULTS

We detected 45 out of 48 (94%) of the single sources, 16 out of 16 (100%) of the primary components, and 12 out of 16 (75%) of the secondary/triple components of the near-infrared binary/multiple objects in our mid-infrared survey. One system, IRS 34, is resolved as a binary in the mid-infrared but remains unresolved at near-infrared wavelengths. The mid-infrared photometry for our target objects is listed in Tables 1–5. Column (1) in each table lists the common name for each source, followed by the objects' J2000.0 coordinates in columns (2) and (3). Column (4) lists the objects'  $10 \mu\text{m}$  flux, or flux upper limit, in janskys. Columns (5) and (6) list the UT observation date and the telescope and instrument combination used.

SEDs were constructed for the binary/multiple objects in Table 1 using the tabulated  $10 \mu\text{m}$  fluxes and  $JHKL$  magnitudes from Haisch et al. (2002, 2004) converted to fluxes in janskys.

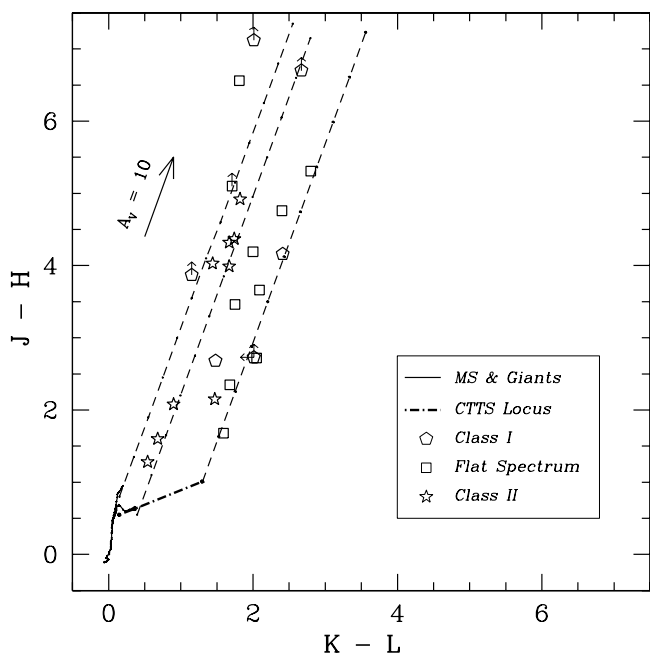


FIG. 1.—*JHKL* color-color diagram for all sources in our mid-infrared binary/multiple survey. All sources are plotted showing their SED classifications. Class I sources are designated with a pentagon, flat-spectrum sources with a square, and Class II sources with a star. We plot the locus of points corresponding to both the unreddened main sequence (MS) and giant branch as a solid line and the CTTS locus as a dot-dashed line. The two leftmost parallel dashed lines define the reddening band for main-sequence stars and are parallel to the reddening vector. The length of the arrow above these lines corresponds to the displacement produced by 10 mag of visual extinction. The rightmost dashed line is parallel to the reddening vector and has its origin at the colors of the reddest TTS.

Each source was classified using the least-squares fit to the slope between 2.2 and 10  $\mu\text{m}$ . We calculated the spectral indices from 2.2 to 10  $\mu\text{m}$  for all observed sources from the relation

$$\alpha = \frac{d \log(\lambda F_\lambda)}{d \log \lambda} \quad (1)$$

in order to quantify the natures of their SEDs (Lada 1987). Our calculated spectral indices are typically good to  $\alpha = \pm 0.3$ , as discussed in § 4. Table 6 lists the 2.2–10  $\mu\text{m}$  spectral indices,  $\alpha$ , for all sources. The classification scheme of Greene et al. (1994) has been adopted in our analysis, as it is believed to correspond well to the physical stages of evolution of YSOs (e.g., André & Montmerle 1994). Class I sources have  $\alpha > 0.3$ , flat-spectrum sources have  $0.3 > \alpha \geq -0.3$ , Class II sources have  $-0.3 > \alpha \geq -1.6$ , and sources with  $\alpha < -1.6$  are Class III YSOs. A Class I object is thought to be one in which the central YSO has attained essentially its entire initial main-sequence mass but is still surrounded by a remnant infall envelope and an accretion disk. Flat-spectrum YSOs represent a transitional class between Class I and Class II objects (e.g., Kikuchi et al. 2002). They are characterized by near-infrared spectra that are strongly veiled by continuum emission from hot, circumstellar dust. Class II sources are surrounded by accretion disks, while Class III YSOs have remnant, or absent, accretion disks. Thus, in this context, the progression from the very red Class I YSO  $\rightarrow$  flat-spectrum  $\rightarrow$  Class II  $\rightarrow$  Class III has frequently been interpreted as representing an evolutionary sequence, even though Reipurth (2000) suggested that a more violent transition from the embedded to the optically bright stages could occur when components are ejected from unstable multiple systems.

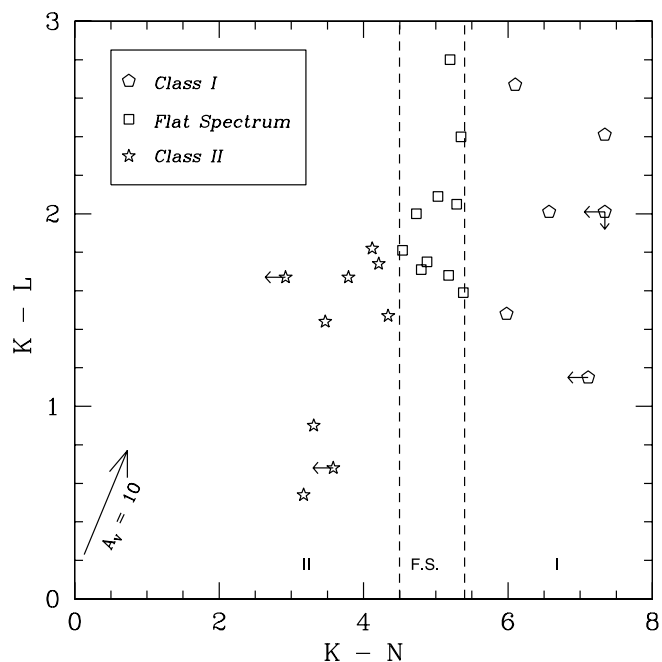


FIG. 2.—Color-color diagram showing the variation of  $K - L$  with  $K - N$  for all sources in Fig. 1; the same symbols are used as in Fig. 1. The area demarcated by the vertical dashed lines indicates the realm of the flat-spectrum sources: the leftmost vertical dashed line represents the  $K - N$  color for a source with  $\alpha = -0.3$  ( $K - N = 4.5$ ), and the rightmost vertical dashed line represents the  $K - N$  color for a source with  $\alpha = +0.3$  ( $K - N = 5.4$ ). The length of the arrow in the diagram corresponds to the displacement produced by 10 mag of visual extinction and has its origin at the photospheric colors of an M4 star ( $K - L = 0.29$ ,  $K - N = 0.13$ ). Arrows on selected objects indicate upper limits on the  $K - L$  or  $K - N$  colors.

In Figure 1 we present the *JHKL* color-color diagram for each individual component of the binary/multiple systems detected in our mid-infrared survey, excepting Cha I T33B and Ced 110 IRS6, for which we do not have *L*-band data, and IRS34, which is unresolved shortward of 10  $\mu\text{m}$ . All sources are plotted showing their SED classifications. Class I sources are designated with a pentagon, flat-spectrum sources with a square, and Class II sources with a star. In the diagram we plot the locus of points corresponding to both the unreddened main sequence and giant branch (Bessell & Brett 1988) as a solid line. The classical TTS (CTTS) locus (Meyer et al. 1997) is shown as a dot-dashed line. The two leftmost parallel dashed lines define the reddening band for main-sequence stars and are parallel to the reddening vector. The length of the arrow above these lines corresponds to the displacement produced by 10 mag of visual extinction. The reddening law of Cohen et al. (1981) has been adopted. All but four of the Class I and flat-spectrum sources lie in the infrared-excess region of the *JHKL* color-color diagram. The four exceptions are GY 263, both components of the IRS 51 system, and the secondary of IRS 54. In addition, only one of the Class II sources, GY 23, lies in the infrared-excess region of the color-color diagram.

In Figure 2 we show the variation of  $K - L$  with  $K - N$  for the same objects as in Figure 1. Sources are plotted with their SED classifications using the same symbols as in Figure 1. The leftmost vertical dashed line represents the  $K - N$  color for a source with  $\alpha = -0.3$  ( $K - N = 4.5$ ), and the rightmost vertical dashed line represents the  $K - N$  color for a source with  $\alpha = +0.3$  ( $K - N = 5.4$ ). Thus, Class I sources should lie to the right of the rightmost vertical dashed line, flat-spectrum sources should lie between the two vertical dashed lines, and Class II sources

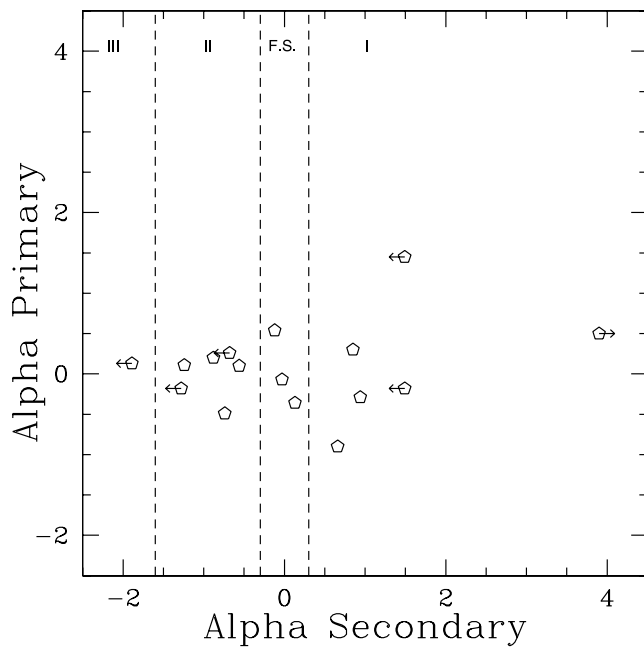


FIG. 3a

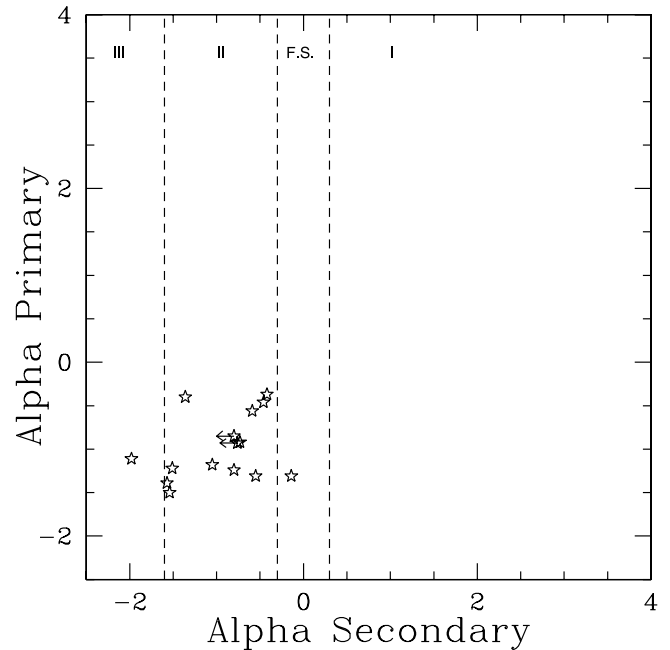


FIG. 3b

FIG. 3.—(a) Plot of the primary's spectral index vs. the secondary's spectral index for our Class I/flat-spectrum sample. (b) Plot of the same quantity for a sample of Class II YSOs from Barsony et al. (2005) and McCabe et al. (2006).

should lie to the left of the leftmost vertical dashed line. The length of the arrow in the diagram corresponds to the displacement produced by 10 mag of visual extinction and has its origin at the photospheric colors of an M4 star ( $K - L = 0.29$ ,  $K - N = 0.13$ ; Bessell & Brett 1988; Ducati et al. 2001).

Visual extinction estimates,  $A_v$ , listed in Table 6 for all except the Class I sources, were determined by dereddening each source in the  $JHK_L$  color-color diagram using the extinction law of Cohen et al. (1981). Complications due to heating and re-processing of both stellar and disk radiation in the remnant infall envelopes preclude accurate dereddening for the Class I sources via this method. For sources in the infrared excess region of the  $JHK_L$  color-color diagram, we dereddened each source to the CTTS locus. For sources to the right of the termination point of the CTTS locus, we used adopted intrinsic colors for the Class II and flat-spectrum sources. For the sources in the reddening band of Figure 1, median intrinsic colors of  $(J - H)_0 = 0.62$  and  $(H - K)_0 = 0.1$  were adopted (Strom et al. 1993). For the Class II sources beyond the termination point of the CTTS locus, we adopted intrinsic colors of  $(J - H)_0 = 0.8$  and  $(H - K)_0 = 0.5$ , while for flat-spectrum sources  $(H - K)_0 = 0.75$  was used (Strom et al. 1993; Greene & Meyer 1995).

## 4. DISCUSSION

### 4.1. SED Characteristics

The composite SEDs for all of our sample YSOs are either Class I or flat-spectrum sources. However, individual source components frequently display Class II, or in one case Class III, spectral indices. In most cases, the SED classes of the primary and secondary components are different, a Class I object being paired with a flat-spectrum source or a flat-spectrum source being paired with a Class II YSO. In one instance (Cha I T33B) we also find a flat-spectrum source paired with a Class III object, and in another (EC92/EC95) a Class I/Class II pairing. Such behavior is not consistent with what one typically finds for

TTs, where the companion of a CTTS also tends to be a CTTS (Prato & Simon 1997; Duchêne et al. 1999). Mixed pairings, however, have been observed among Class II YSOs previously (Ressler & Barsony 2001; McCabe et al. 2006).

We plot the primary's spectral index versus the secondary's spectral index for our Class I/flat-spectrum sample in Figure 3a. For comparison, we show the same plot in Figure 3b for Class II YSOs from data in Barsony et al. (2005) and McCabe et al. (2006). For a given primary spectral index, there is a larger spread in the spectral indices of the secondaries among the Class I/flat-spectrum sample compared to the Class II sample. Thus, there appears to be a higher proportion of mixed Class I/flat-spectrum systems (79%) than there are of mixed classical and weak-lined T Tauri systems (25%) (Hartigan & Kenyon 2003; Prato et al. 2003; Barsony et al. 2005; McCabe et al. 2006). Allowing for the  $\alpha = \pm 0.3$  error in our calculated spectral indices, we find the proportion of mixed Class I/flat-spectrum systems (65%) remains higher than that of mixed classical and weak-lined T Tauri systems (42%). Given the low likelihood of misclassification of Class I and Class II YSOs as discussed below, this demonstrates that the envelopes of Class I/flat-spectrum systems are rapidly evolving during this evolutionary phase, although they may still be coeval. Although the central objects of Class I and flat-spectrum sources (Doppmann et al. 2005; Covey et al. 2005) and even Class II YSOs (Kenyon et al. 1998; White & Hillenbrand 2004) have similar stellar and accretion properties, their envelope properties clearly differ.

In general, the individual components of a given binary/multiple system suffer very similar extinctions,  $A_v$ , suggesting that most of the line-of-sight material is either in the foreground of the molecular cloud or circumbinary. One notable exception is the GY 244/WL 5 pair, whose  $A_v$  values differ by *at least* 11 mag. While their projected separation is  $\sim 1100$  AU (Haisch et al. 2004), it is possible that GY 244 and WL 5 represent a chance projection. WL 5 is known to be one of the most heavily extinguished infrared sources in the  $\rho$  Oph cloud core (André et al. 1992), consistent with our measured value of  $A_v \geq 44.0$ . Our

results are consistent with those of previous authors, who find WL5 to be a Class III YSO seen through large amounts of foreground cloud material (André & Montmerle 1994 and references therein; Bontemps et al. 2001).

The superiority of using the *KLN* color-color diagram to specify the SED classes of YSOs relative to the traditionally used *JHKL* color-color diagram is evident on comparison of Figures 1 and 2. In the *KLN* color-color diagram of Figure 2, the Class II, flat-spectrum, and Class I objects are very cleanly separated, whereas they remain relatively confused in the *JHKL* color-color diagram of Figure 1. Furthermore, Class II sources cannot be distinguished from reddened background stars in Figure 1 (all but one lie in the reddening band), whereas they all lie in a clearly demarcated region in Figure 2.

Source variability may affect the SED classification of an object in the sense that, in general, the near- and mid-infrared fluxes for a given object in this survey were not acquired simultaneously. To estimate the possible effect of source variability on SED class, we note that YSO variability in the *K* band has been observed at amplitudes ranging from 0.32 to 0.65 mag in Oph (Barsony et al. 1997) and from 0.15 to 2.2 mag in Ser with typical amplitudes  $< 0.75$  mag (Kaas 1999) and with typical amplitudes of 0.2 mag in Orion A (Carpenter et al. 2001). For most of our source sample, the *L*-band magnitudes presented in Table 6 are the only ones available, so we cannot estimate the typical *L*-band variations one might observe in the YSO populations. Our *L*-band photometric errors are typically 0.1–0.2 mag for the fainter sources. In a recent large-scale mid-infrared survey of Oph YSOs, at least 20% of all embedded sources are known to have significant flux variations, ranging from 0.2 to 1.8 mag at *N* band, with typical amplitudes  $< 0.5$  mag (Barsony et al. 2005). Using the typical variations in magnitude at *K* and *N* band, if a source varies in such a fashion that it becomes bluer, i.e., increasing  $2 \mu\text{m}$  emission and decreasing  $10 \mu\text{m}$  emission,  $\alpha$  could vary by  $-0.3$ . If a source varies in the sense of becoming redder, that is, its  $2 \mu\text{m}$  flux is decreasing as its  $10 \mu\text{m}$  flux increases, then  $\alpha$  could vary by  $+0.3$ . These are worst-case effects on misclassifying an object's SED class.

Referring to Figure 1, there are two Class I and two flat-spectrum sources that lie blueward of the reddening band. The position of these sources in the *JHKL* color-color diagram cannot be explained using spherically symmetric radiative transfer models for the embedded YSOs. Two-dimensional radiative transfer models, however, can reproduce the location of these YSOs in Figure 1 through a combination of the presence of outflow cavities carved out of the infall or remnant infall envelopes and inclination effects (Whitney et al. 2003a, 2003b). The two Class I sources that lie to the left of the reddening band in Figure 1 are the secondary components of IRS 51 ( $J - H \Rightarrow 7.20$ ,  $K - L = 2.01$ ) and IRS 54 ( $J - H \Rightarrow 3.87$ ,  $K - L = 1.15$ ). IRS 51 has been examined in detail by Haisch et al. (2002), who concluded that the mid-infrared secondary may be a bright knot in the molecular outflow from IRS 51 (Bontemps et al. 1996) along a north-south cavity seen in scattered light at *K* band rather than a true YSO. We note, however, that Duchêne et al. (2004) consider the secondary to IRS 51 to be a real source, as it appears indistinguishable from a point source in their image of the system. The secondary to IRS 54 was undetected in our survey. Its flux upper limit is consistent with either a Class I or later SED class YSO ( $\alpha \leq +1.49$ ). Two flat-spectrum sources, the primary of IRS 51 ( $J - H = 6.56$ ,  $K - L = 1.81$ ) and GY 263 ( $J - H \Rightarrow 5.10$ ,  $K - L = 1.71$ ), also lie to the left of the reddening band in Figure 1. With a spectral index of  $\alpha = -0.29$ , the primary of IRS 51 is right at the border line between flat-

spectrum and Class II classification. Its designation as a flat-spectrum source is supported by Barsony et al. (2005), who derive a spectral index of  $+0.13$  for the IRS 51 primary. In the case of GY 263, Barsony et al. (2005) derive a spectral index of  $\alpha = -0.4$  for the source, making it a Class II YSO.

Whereas the sources discussed above lie in regions of the *JHKL* color-color diagram that obviate correct determination of their SED classes, in the *KLN* color-color diagram of Figure 2 they all lie at their expected locations. In Figure 2 there is a clear progression from the very red Class I YSO  $\rightarrow$  flat spectrum  $\rightarrow$  Class II.

While near-to mid-infrared colors generally reflect the evolutionary state of a given object, we note that there may be instances in which the SED class does not yield the correct evolutionary state. For example, since the flux at  $2 \mu\text{m}$  suffers heavier extinction than the  $10 \mu\text{m}$  flux, a Class II YSO seen through a large amount of foreground obscuration may show a Class I or flat-spectrum SED. Orientation effects may also be important, since a nearly pole-on Class I source may display a SED similar to an edge-on Class II object (Whitney et al. 2003a). Nevertheless, protostellar envelopes extinct the stellar flux over a much larger range of solid angle than disks. Assuming a random distribution of orientations in two dimensions and the most likely orientation to be  $45^\circ$ , if we assume an inclination angle in the range  $45^\circ \leq i \leq 135^\circ$ , then 70% of Class I YSOs will be properly classified. Furthermore, if one assumes a random distribution in three dimensions of disk orientations, the probability of observing a disk edge-on ( $85^\circ \leq i \leq 95^\circ$ ) is 9%. Thus, only 9% of Class II sources would be improperly classified as Class I (B. Whitney 2006, private communication). Furthermore, the SEDs of Class I and Class II YSOs do look distinctly different, with Class I sources exhibiting larger far-infrared excesses.

The rigorously correct way to determine an object's evolutionary state is to obtain multiwavelength imaging data for each source and quantitatively compare these data to models produced using three-dimensional radiative transfer codes (Whitney et al. 2003a). For example, Osorio et al. (2003) have self-consistently modeled each component of the Class I binary L1551 IRS 5, adopting a flattened infalling envelope surrounding a circum-binary disk. A wealth of observations for this system provide additional constraints for any viable source models: *Infrared Space Observatory (ISO)* imaging, spectroscopy of the water ice feature with SpeX, and high-resolution VLA imaging at 7 mm resolving the binary disks. The results show that a flattened-envelope collapse model is required to explain simultaneously the large-scale fluxes and the water ice and silicate features. The circumstellar disks are optically thick in the millimeter range and are inclined so that their outer parts hide the emission along the line of sight from their inner parts. Furthermore, these disks have lower mass accretion rates than the infall rate of the envelope. Unfortunately, such multiwavelength data are not available for our sources; thus, we must rely on the spectral indices as an indicator of YSO evolutionary states.

#### 4.2. Notes on Selected Sources

**03260+3111:** This source was observed to be binary in the near-infrared with a  $3''.62$  separation and a position angle of  $47^\circ 9'$  (Haisch et al. 2004). In the present survey only the *K*-band primary is detected. The system appears extended with a fan-shaped nebulosity in the mid-infrared. Based on an optical and near-infrared imaging survey, Magnier et al. (1999) have classified 03260+3111 as a flat-spectrum YSO. Our mid-infrared photometry suggests that the primary is a Class II object, while our upper limit for the flux of the secondary suggests that it is at least a Class II YSO.

**Ced 110 IRS 6:** The primary of this binary system (separation = 1".95, P.A. = 95°.6) has the largest visual extinction ( $A_v \geq 51.0$ ) in our survey. With a spectral index of +0.30, it is right on the border line between flat-spectrum and Class I YSOs and, therefore, may in fact be a Class I object. If so, Ced 110 IRS 6 would represent the only binary in our survey in which both components are Class I. Mid- and far-infrared observations with ISOCAM and ISOPHOT suggest that most of the flux density is associated with the primary component of the binary (Lehtinen et al. 2001).

**ISO-Cha I 97:** ISO-Cha I 97 was detected as a single star in our near-infrared imaging survey of binary/multiple Class I and flat-spectrum YSOs (Haisch et al. 2004). Our mid-infrared observations have revealed that this source is in fact binary (separation = 2".05, P.A. = 72°.6). Our  $5\sigma$   $K$ -band sensitivity limit of  $\sim 18.5$  combined with our  $10\ \mu\text{m}$  flux yields a lower limit to the spectral index of the secondary component of ISO-Cha I 97 of  $\alpha \geq +3.9$  (the primary component has a spectral index  $\alpha = +0.50$ ). This very steep spectral index places the secondary of ISO-Cha I 97 in a class of YSO that has heretofore been rarely known, i.e., those with  $\alpha > +3$ . Three such objects have been recently reported, the Class 0 object Cep E mm (Noriega-Crespo et al. 2004), source X<sub>E</sub> in R CrA (Hamaguchi et al. 2005), and source L1448 IRS 3(A) (Ciardi et al. 2003; Tsujimoto et al. 2005). Further very steep spectrum YSOs are expected to be discovered with the *Spitzer Space Telescope*.

**IRS 34:** As is the case for ISO-Cha I 97, IRS 34 was observed to be a single source in the near-infrared (Haisch et al. 2004) but binary in the mid-infrared (Barsony et al. 2005). The components of IRS 34 are separated by only 0".31 (P.A. = 236°.0) and therefore could not be resolved in our near-infrared survey. For this reason, we are also unable to construct SEDs for the individual components of IRS 34.

Finally, we note that we did not detect the secondaries of the Cha I T33B, IRS 48, IRS 54, and GY 51 binary/multiple sources in the mid-infrared. We derived upper limits for the SED classifications for these components based on our mid-infrared flux upper limits. These classifications are likely rather firm for the secondaries of Cha I T33B and IRS 48; however, given the large extinctions observed toward IRS 54 ( $A_v > 25$  mag; Haisch et al. 2004) and GY 51 ( $A_v \simeq 30$ ), the SED classifications for these components are less secure. The secondary of IRS 54 appears to be a Class I YSO. Accounting for the extinction toward GY 51 (see Duchêne et al. [2004] for a  $K$ -band image of this triple system), the components of this system would become Class II–III, Class III, and Class II for the primary, secondary, and third components, respectively.

## 5. SUMMARY AND CONCLUSIONS

We have obtained new mid-infrared observations of 65 Class I/flat-spectrum objects in the Perseus, Taurus, Chamaeleon I and II,  $\rho$  Ophiuchi, and Serpens dark clouds. These objects represent a subset of the YSOs from our previous near-infrared multiplicity surveys (Haisch et al. 2002, 2004). We detected 45 out of 48 (94%) of the single sources, 16 out of 16 (100%) of the primary

components, and 12 out of 16 (75%) of the secondary/triple components of the binary/multiple objects surveyed. The tight mid-infrared binary, IRS 34, remains unresolved at near-infrared wavelengths.

While the composite SEDs for all of our sample YSOs are either Class I or flat spectrum, individual source components may display Class II or, in one case, Class III spectral indices. The SED classes of the primary and secondary components are frequently different. For example, a Class I object may be found to be paired with a flat-spectrum source, or a flat-spectrum source paired with a Class II YSO. Such behavior is not consistent with what one typically finds for TTSSs, where the companion of a CTTS also tends to be a CTTS (Prato & Simon 1997; Duchêne et al. 1999). Mixed pairings, however, have been previously observed among Class II YSOs (Ressler & Barsony 2001; McCabe et al. 2006).

Based on an analysis of the spectral indices of the individual binary components, there appears to be a higher proportion of mixed Class I/flat-spectrum systems (65%–80%) than that of mixed classical and weak-lined T Tauri systems (25%–40%). This demonstrates that the envelopes of Class I/flat-spectrum systems are rapidly evolving during this evolutionary phase, although they may still be coeval.

In general, the individual binary/multiple components suffer very similar extinctions,  $A_v$ , suggesting that most of the line-of-sight material is either in the foreground of the molecular cloud or circumbinary. However, the GY 244/WL 5 pair, whose  $A_v$  values differ by 11 mag, is a notable exception. If the projected separation of this pair ( $\sim 1100$  AU) is equivalent to its physical separation, then this system could easily be gravitationally bound. However, it is also possible that GY 244 and WL 5 represent a chance projection.

ISO-Cha I 97 was detected as a single star in our near-infrared imaging survey of binary/multiple Class I and Flat-Spectrum YSOs (Haisch et al. 2004). Our mid-infrared observations have revealed that this source is in fact binary. Combining our  $K$ -band sensitivity limit from Haisch et al. (2004) with our  $10\ \mu\text{m}$  flux yields a lower limit to the spectral index of the secondary component of ISO-Cha I 97 of  $\alpha \geq +3.9$ . This very steep spectral index places the secondary of ISO-Cha I 97 in a class of YSO that has heretofore been rarely known, i.e., those with  $\alpha > +3$ . Further very steep spectrum YSOs are expected to be discovered with *Spitzer*.

We thank the Magellan Observatory staff for their outstanding support in making our observations possible. K. E. H. gratefully acknowledges partial support from NASA Origins grant NAG5-11905 to Ray Jayawardhana. M. B. acknowledges NSF grant AST 02-06146 and NASA LTSA grant NAG5-8933 to Barbara Whitney, which made her contributions to this work possible, as well as a NASA Summer Faculty Fellowship held at NASA's Ames Research Center during the summers of 2003–2004. T. P. G. acknowledges support from NASA Origins of Solar Systems grant 344-37-22-11.

## REFERENCES

- Abt, H. A., & Levy, S. 1976, *ApJS*, 30, 273  
 Adams, F. C., Lada, C. J., & Shu, F. H. 1987, *ApJ*, 312, 788  
 ———. 1988, *ApJ*, 326, 865  
 André, P., Deeney, B. D., Phillips, R. B., & Lestrade, J.-F. 1992, *ApJ*, 401, 667  
 André, P., & Montmerle, T. 1994, *ApJ*, 420, 837  
 Barsony, M., & Kenyon, S. J. 1992, *ApJ*, 384, L53  
 Barsony, M., Kenyon, S. J., Lada, E. A., & Teuben, P. 1997, *ApJS*, 112, 109  
 Barsony, M., Koresko, C., & Matthews, K. 2003, *ApJ*, 591, 1064  
 Barsony, M., Ressler, M. E., & Marsh, K. 2005, *ApJ*, 630, 381  
 Bessell, M. S., & Brett, J. M. 1988, *PASP*, 100, 1134  
 Bontemps, S., André, P., Terebey, S., & Cabrit, S. 1996, *A&A*, 311, 858  
 Bontemps, S., et al. 2001, *A&A*, 372, 173

- Brandner, W., & Zinnecker, H. 1997, *A&A*, 321, 220
- Carpenter, J., Hillenbrand, L. A., & Skrutskie, M. F. 2001, *AJ*, 121, 3160
- Chick, K. M., & Cassen, P. 1997, in *IAU Symp. 182, Low-Mass Star Formation from Infall to Outflow*, ed. F. Malbet & A. Castets (Grenoble: Obs. Grenoble), 207
- Ciardi, D. R., Telesco, C. M., Williams, J. P., Fisher, R. S., Packham, C., Piña, R., & Radomski, J. 2003, *ApJ*, 585, 392
- Cohen, J. G., Frogel, J. A., Persson, S. E., & Elias, J. H. 1981, *ApJ*, 249, 481
- Covey, K. R., Greene, T. P., Doppmann, G. W., & Lada, C. J. 2005, *AJ*, 129, 2765
- de Lara, E., Chavarría-K., C., & Lopez-Molina, G. 1991, *A&A*, 243, 139
- Doppmann, G. W., Greene, T. P., Covey, K. R., & Lada, C. J. 2005, *AJ*, 130, 1145
- Ducati, J. R., Bevilacqua, C. M., Rembold, S. B., & Ribeiro, D. 2001, *ApJ*, 558, 309
- Duchêne, G., Bouvier, J., Bontemps, S., André, P., & Motte, F. 2004, *A&A*, 427, 651
- Duchêne, G., Monin, J.-L., Bouvier, J., & Ménard, F. 1999, *A&A*, 351, 954
- Duquennoy, A., & Mayor, M. 1991, *A&A*, 248, 485
- Fischer, D. A., & Marcy, G. W. 1992, *ApJ*, 396, 178
- Ghez, A. M., McCarthy, D. W., Patience, J., & Beck, T. 1997, *ApJ*, 481, 378
- Ghez, A. M., Neugebauer, G., & Matthews, K. 1993, *AJ*, 106, 2005
- Girart, J. M., Curiel, S., Rodríguez, L. F., Honda, M., Cantó, J., Okamoto, Y. K., & Sako, S. 2004, *AJ*, 127, 2969
- Greene, T. P., & Meyer, M. R. 1995, *ApJ*, 450, 233
- Greene, T. P., Wilking, B. A., André, P., Young, E. T., & Lada, C. J. 1994, *ApJ*, 434, 614
- Haisch, K. E., Jr., Barsony, M., Greene, T. P., & Ressler, M. 2002, *AJ*, 124, 2841
- Haisch, K. E., Jr., Greene, T. P., Barsony, M., & Stahler, S. W. 2004, *AJ*, 127, 1747
- Hamaguchi, K., Corcoran, M. F., Petre, R., White, N. E., Stelzer, B., Nedachi, K., Kobayashi, N., & Tokunaga, A. T. 2005, *ApJ*, 623, 291
- Hartigan, P., & Kenyon, S. J. 2003, *ApJ*, 583, 334
- Hartigan, P., Strom, K. M., & Strom, S. E. 1994, *ApJ*, 427, 961
- Herbig, G. H. 1998, *ApJ*, 497, 736
- Hoffmann, W. F., Hora, J. L., Fazio, G. G., Deutsch, L. K., & Dayal, A. 1998, *Proc. SPIE*, 3354, 647
- Kaas, A. A. 1999, *AJ*, 118, 558
- Kenyon, S. J., Brown, D. I., Tout, C. A., & Berlind, P. 1998, *AJ*, 115, 2491
- Kenyon, S. J., Calvet, N., & Hartmann, L. 1993, *ApJ*, 414, 676
- Kenyon, S. J., & Hartmann, L. 1995, *ApJS*, 101, 117
- Kikuchi, N., Nakamoto, T., & Ogochi, K. 2002, *PASJ*, 54, 589
- Knude, J., & Høg, E. 1998, *A&A*, 338, 897
- Lada, C. J. 1987, in *Star-Forming Regions*, ed. M. Peimbert & J. Jugaku (Dordrecht: Reidel), 1
- Lehtinen, K., Haikala, L. K., Mattila, K., & Lemke, D. 2001, *A&A*, 367, 311
- Liu, M. C., et al. 1996, *ApJ*, 461, 334
- Looney, L. W., Mundy, L. G., & Welch, W. J. 1997, *ApJ*, 484, L157
- . 2000, *ApJ*, 529, 477
- Magnier, E. A., Volp, A. W., Laan, K., van den Ancker, M. E., & Waters, L. B. F. M. 1999, *A&A*, 352, 228
- Mathieu, R. D. 1994, *ARA&A*, 32, 465
- McCabe, C., Ghez, A. M., Prato, L., Duchêne, G., Fisher, R. S., & Telesco, C. 2006, *ApJ*, 636, 932
- Meyer, M. R., Calvet, N., & Hillenbrand, L. A. 1997, *AJ*, 114, 288
- Noriega-Crespo, A., Moro-Martín, A., Carey, S., Morris, P. W., Padgett, D. L., Latter, W. B., & Muzerolle, J. 2004, *ApJS*, 154, 402
- Osorio, M., D'Alessio, P., Muzerolle, J., Calvet, N., & Hartmann, L. 2003, *ApJ*, 586, 1148
- Prato, L., Greene, T. P., & Simon, M. 2003, *ApJ*, 584, 853
- Prato, L., & Simon, M. 1997, *ApJ*, 474, 455
- Reipurth, B. 2000, *AJ*, 120, 3177
- Reipurth, B., & Zinnecker, H. 1993, *A&A*, 278, 81
- Ressler, M. E., & Barsony, M. 2001, *AJ*, 121, 1098
- Ressler, M. E., Werner, M. W., Van Clever, J., & Chou, H. A. 1994, *Exp. Astron.*, 3, 277
- Simon, M., et al. 1995, *ApJ*, 443, 625
- Strom, K. M., Strom, S. E., & Merrill, K. M. 1993, *ApJ*, 412, 233
- Tsujimoto, M., Kobayashi, N., & Tsuboi, Y. 2005, *AJ*, 130, 2212
- White, R. J., & Hillenbrand, L. A. 2004, *ApJ*, 616, 998
- Whitney, B. A., Wood, K., Bjorkman, J. E., & Cohen, M. 2003a, *ApJ*, 598, 1079
- Whitney, B. A., Wood, K., Bjorkman, J. E., & Wolff, M. J. 2003b, *ApJ*, 591, 1049
- Whittet, D. C. B., Prusti, T., Franco, G. A. P., Gerakines, P. A., Kilkenney, D., Larson, K. A., & Wesselius, P. R. 1997, *A&A*, 327, 1194